Research Square

Preprints are preliminary reports that have not undergone peer review.
They should not be considered conclusive, used to inform clinical practice,
or referenced by the media as validated information.

Salt Marsh Morphological Evolution Under Plant Species Invasion

Xinchen Wang

xcwang@hhu.edu.cn

Hohai University https://orcid.org/0000-0003-0972-2897

Pei Xin

State Key Laboratory of Hydrology-Water Resources and Hydraulic Engineering

Hong Zhang

Griffith University - Gold Coast Campus

Lucheng Zhan

Hohai University

Congcong Lao

Hohai University

Research Article

Keywords: Plant invasion, tidal creeks, morphological characteristic, the Yangtze Estuary and the Jiuduansha Shoal

Posted Date: June 7th, 2023

DOI: https://doi.org/10.21203/rs.3.rs-2856772/v1

License: This work is licensed under a Creative Commons Attribution 4.0 International License.
Read Full License

Version of Record: A version of this preprint was published at Estuaries and Coasts on March 14th, 2024.
See the published version at https://doi.org/10.1007/s12237-024-01346-7.

Abstract

Species invasion in salt marsh wetlands is known to disturb the balance of biotic and abiotic ecosystems (e.g., changing material exchange cycles and community structure). However, its influence on the morphological evolution of salt marshes is not yet understood in depth. This study investigates the long-term temporal and spatial distributions of an invasive plant—*Spartina alterniflora* (*S. alterniflora*)—and its morphological characteristics in Yangtze Estuary by remote sensing imagery interpretation, tidal creek extraction, regional statistical analysis, and proximity analysis. The invaded site shows an area of *S. alterniflora* with a 35-fold increase from the start to the end of its initiation phase; it is the second biggest species in the study area. It is found that species invasion not only limited the expansion of native pioneer vegetation but also changed bio-geomorphic feedback loops. With the influence of plant invasion, median tidal creek lengths decreased and the median tidal creek sinuosity ratio remained stable, between 1.06 and 1.07 in the subarea. The method used here is adaptable to other salt marshes. The findings from this study can provide practical guidance for the restoration of native salt marshes in the estuary and thus control the spread of invasive species.

1. Introduction

Coastal wetlands, a type of wetland ecosystem, consist of salt marsh and mangroves. They have a significant carbon sequestration rate and long-term sustainable carbon sequestration capacity. The United Nations estimates that half of the carbon sequestered by living organisms takes place in “blue-carbon” wetlands. Coastal wetlands are an important type of “blue-carbon” wetland. These carbon-rich ecosystems help to reduce carbon dioxide (CO_2) emissions, moderate climate change, serve as a resource for local people, and achieve carbon neutrality (Jimenez et al. 2012; Mcleod et al. 2011; F. Wang et al. 2020).

These highly productive blue carbon ecosystems face accelerating rates of sea-level rise, human reclamation activities, and salt intrusion, and are at considerable risk of degradation (Andrea D'Alpaos 2011). The area of global native salt marshes is estimated to have decreased by about half over the past century (Goulden et al. 2007; Kennish 2001; Kirwan and Megonigal 2013; W. Wu et al. 2018). The reduction of coastal wetlands per square kilometer is equivalent to the annual reduction of 0.22 Gg C sequestration, which is also equivalent to the annual increase of CO_2 emissions from burning 3.36 × 105 L gasoline (Davis et al. 2015). Therefore, there is an urgent need to protect and preserve the salt marsh ecosystem.

Recently, species invasion has gained the attention of experts and coastal wetland decision-makers. *Spartina alterniflora* (*S. alterniflora*), or smooth cordgrass, is native to the intertidal coastal wetlands of North America (Christian Schwarz et al. 2016). It has been introduced mostly to the east coast of China (An et al. 2007), New Zealand (Hubbard and Partridge 1981), and along the Pacific coast of North America (Frenkel and Boss 1988). It is estimated that the area of *S. alterniflora* in China has now reached 546 km^2, an increase of 502 km^2 compared with 1990. It is mainly distributed in the provinces alonge the

east coast of China (Mao et al. 2019). These newly expanded *S. alterniflora* wetlands have largely encroached on the original coastal tidal flats (Mao et al. 2019). *S. alterniflora*'s global distribution has occurred for several reasons, including its deliberate spread for erosion control and accretion for land reclamation, as well as accidental introductions via agriculture and ship ballasts (Callaway and Josselyn 1992; Li et al. 2009). *S. alterniflora* is strongly adaptable and tolerant, and possesses ecosystem engineering capabilities (van Hulzen et al. 2007) owing to its dense and stiff above-ground shoots. These provide hydrodynamic friction, reduce flow velocities, and hence increase mineral sediment accretion within its patches. The above-ground roots combine with the below-ground roots to reduce erosion and contribute to organic matter accretion (Bouma et al. 2005; Neubauer 2008; Nyman et al. 2006; Vandenbruwaene et al. 2011).

Invasive species' general effects on the ecosystem process can be both biotic and abiotic (Fei et al. 2014; Strayer et al. 2006; Theoharides and Dukes 2007). Biotic effects include competition with native flora (Frenkel and Boss 1988; Huang and Zhang 2007), the reduction of intertidal native fauna biodiversity(Chen et al. 2004; Li et al. 2009), such as benthos, and altered habitat quality for shorebird and wading birds (Goss-Custard and Moser 1988; Ma et al. 2007). Abiotic effects include species invasion that reduces flow velocity and affects threshold shear stress, which results in trapping and soil expansion. Invading species lead to elevation change driven by organic production, accumulation, and decomposition, assumed to be proportional to biomass (A. D'Alpaos et al. 2006). Moreover, not only has this resulted in altered sediment quality and quantity (Kakeh et al. 2016; Yang et al. 2008), but it has also changed pioneer zone composition and expansion rates in salt marsh systems (Ge et al. 2013; Rosso et al. 2006).

Many studies discuss abiotic environments in coastal wetlands, especially the morphological processes of salt marshes)(Gong et al. 2021; Lao et al. 2022; Quan et al. 2016; Sheehan and Ellison 2014; B. Zhao et al. 2019; Zhu et al. 2012). Research has identified lower tidal creek curvatures around invasion species (*S. alterniflora*) compared with curvatures closer to native species (*Phragmites australis* and *Suaeda salsa*) in the Yellow River Estuary; plant gathering promotes tidal creek networks achieving equilibrium (Fan et al. 2020; Gong et al. 2021). In addition, scholars have compared the differences in tidal creek networks between well-developed vegetation zones and poorly vegetated covered zones, determining that the number, length, and depth of tidal creeks are higher in the vegetated zone in the central coastal region of Jiangsu, China (B. Zhao et al. 2019). Moreover, tidal creek drainage decreased and sediment composition was altered after *S. alterniflora* expanded in the south of eastern Chongming Island, in the Yangtze River Estuary.

Although the effects of *S. alterniflora* invasion on short-term geomorphology processes in a vertical column have been examined, few studies have investigated its influences on long-term geomorphology processes in varied horizontal spatial scales (Sheehan and Ellison 2014; Xiao et al. 2010). Tidal creek networks are important channels for transporting water, sand materials, nutrients, and substances to the upper parts of tidal flats, and are the most active geomorphic unit linking estuarine and marine

environments(Kearney and Fagherazzi 2016; Marani et al. 2002; Y. Wu et al. 2020; Xin et al. 2022; Zhao et al. 2022). However, the effects of *S. alterniflora* invasion on tidal creek network expansion remain unclear.

Using the salt marshes in the mesotidal Yangtze River Estuary as a case study, we investigate the salt marsh evolution under the influence of vegetation invasion, as well as the bio-geomorphic feedback between salt marshes and invasive vegetation. Our specific objectives are (1) to explore and estimate the spatial and temporal variation of invasive plant coverage; (2) to analyze the long-term morphological characteristics of a salt marsh system; and (3) to investigate how invasive plants influence morphological features, especially tidal creek networks.

2. Research domain

The study area is located in the Jiuduansha Wetland National Nature Reserve with the geographical coordinates of 31°03'–3°17' N and 121°46'–122°15' E, at the estuary of the Yangtze River (Fig. 1), China. The JiuDuanSha Shoal (JDS shoal) of the Yangtze Estuary has an eastern Asian monsoon climate with an average annual water temperature ranging from 15.2–15.8°C. It has an average annual precipitation of 1,022 mm, and an average humidity of approximately 82%. The tides are irregular and semidiurnal with an average tidal amplitude of 1.96–3.08 m. JDS shoal is a shoal located between the North Passage and the South Passage at the estuary of the Yangtze Estuary, covering an area of 36 km2 salt marshes, 94 km2 tidal flats, and 300 km2 subtidal soft bottoms (Quan et al. 2011). Yangtze River discharge decreased after construction of the Three Gorges Dam water storage from 2003 to 2013, with the decrease of annual sediment discharge from 2.06 Mt to 1.17 Mt. It is worth mentioning that the North Passage Deep Navigation Channel Project contrasted from 2001 to 2011. *S. alterniflora* was intentionally introduced into the shoal for rapid sediment accretion in the late 1990s. Since then, the exotic plant has rapidly excluded two native plants: *Phragmites australis* (*P. australis*) and *Scirpus mariqueter* (*S. mariqueter*). *S. alterniflora* is distributed in the coastal wetlands with elevations above 2.5–2.9 m.

Figure 1 (located here)

JDS shoal is composed of the Shangsha Shoal, the Zhongsha Shoal, and the Xiasha Shoal (Fig. 2). The distribution and development of tidal creek networks in JDS shoal are different, and native and invasive vegetation in different areas varies. Therefore, JDS shoal is divided into three subareas from the northwest to the southeast, and includes six zones (Fig. 2). Zone 1 belongs to the entrance zone of the Yangtze Estuary; Zones 2, 3 and 4 belong to the transition zones; and Zones 5 and 6 belong to the coastal zones.

Figure 2 (located here)

3. Methodology

3.1 Data Set

The extraction of tidal creeks and halophytic vegetation is derived from remote satellite imagery. Annual satellite images in Landsat 5-TM, Landsat 7 ETM+, and Landsat 8OLI from Google Earth Engine (GEE, https://earthengine.google.com/), and HJ-1A from the China Centre for Resources Satellite Data and Application (CRESDA, https://data.cresda.cn/#/home) from January 1, 1996 to January 1, 2021 were used. The bathymetry of nearby water was measured by the Yangtze Estuary Waterway Administration from 1959 to 2021. Water Resources of the People's Republic of China provided the physical data, including annual runoff, annual sediment discharge, current velocity, sediment concentration, and tidal level. Table 1 lists the available data.

Table 1
Relevant parameters in Tingalpa Reservoir during four storm events

Data	Source	Period
Satellite Image	Landsat 5-TM, Landsat 7-TM, Landsat 8-TM (Google Earth) and HJ-1A (CRESDA)	1996–2020
Bathymetry	Yangtze Estuary Waterway Administration	1959–2021
Annual runoff	Water Resources of the People's Republic of China	1950–2018
Annual sediment discharge		1950–2018
Current velocity		2001–2018
Sediment concentration		2001–2018
Tidal level		2001–2018

3.2 Zonation

The coastal tidal flat can be divided into three parts according to their locations, including terrestrial vegetation above the highest astronomical tidal level, salt marsh between high tidal level to the highest astronomical tidal level, and mudflat between low tidal level and high tidal level (Fig. 3). *S. mariqueter* and *P. australis* are two types of major native vegetation in JDS shoal. *S. alterniflora* invades the front of salt marshes and then also invades the area of native species. To analyze the spatial distribution of morphological and vegetation characteristics, the study domain was divided into six zones (Fig. 2). There are two zones in Shangsha Shoal, one in the Zhongsha Shoal, and three in the Xiasha Shoal. Zone 1 is the entrance zone of the Yangtze Estuary; Zones 2 and 3 are the transition zones; and Zones 4, 5, and 6 are the coastal zones. The relevant analysis results of each zone's characteristics as a tidal creek system and vegetation invasion are presented in Section 4.2.

Figure 3 (located here)

3.2 Extraction of Tidal Creek Network and Tracking Species Invasion

In this study, we used time series Landsat data sets, VHSR images from Google Earth, and in situ data to identify and map tidal creeks and saltmarshes on the Jiuduansha Shoal. We used all available Landsat 5/7/8 surface reflectance (SR) products between January 1, 1996 and January 1, 2021. These were archived in Google Earth Engine (GEE), a popular cloud computing platform for planetary-scale remote sensing analysis (Gorelick et al. 2017). The SR data sets have been atmospherically corrected through the Landsat Ecosystem Disturbance Adaptive Processing System algorithm and the Landsat Surface Reflectance Code algorithm. Poor-quality observations, including clouds, cirrus, and cloud shadows were identified according to the pixel quality assessment generated from the CFMask algorithm. All Landsat image pre-processing tasks were conducted on the GEE platform. The time series Landsat SR data with high tidal levels and good-quality observations were used to calculate four indices: normalized difference water index (I_{NDW}), modified normalized difference water index (I_{MNDW}), normalized difference vegetation index (*NDVI*), and enhanced vegetation index (*EVI*). *NDWI* and *MNDWI* identify water bodies. *NDVI* and *EVI* identify coastal vegetation. These four indices are calculated using the following equations:

$$NDWI = \frac{B_{Green} - B_{NIR}}{B_{Green} + B_{NIR}} \quad (1)$$

$$MNDWI = \frac{B_{Green} - B_{SWIR}}{B_{Green} + B_{SWIR}} \quad (2)$$

$$NDVI = \frac{B_{NIR} - B_{Red}}{B_{NIR} + B_{Red}} \quad (3)$$

$$EVI = 2.5 \times \frac{B_{NIR} - B_{Red}}{B_{NIR} + 6 \times B_{Red} - 7.5 \times B_{Blue} + 1} \quad (4)$$

where B_{Blue},B_{Green}, B_{Red}, B_{NIR}, and B_{SWIR} are the SR values of blue (450–520 nm), green (520–600 nm), red (630–690 nm), near-infrared (NIR: 760–900 nm), and shortwave-infrared (SWIR: 1550–1750 nm) bands. These indices are used as independent variables to predict ground object types. Based on VHSR (very high spatial resolution) images from Google Earth and field survey data, samples (mudflat, tidal creeks, and salt marsh vegetation) are made and used for random forest model training. After training, the model can output classification maps; validation data and results from other studies are used to manually correct the classification results in ArcGIS 10.6.

The characteristic parameters of the tidal creek network, including tidal creek order, length, number, sinuosity ratio, and drainage ratio, are analyzed in this research. In accordance with the Horton-Strahler principle (Horton 1945), tidal creeks without branches are defined as Order 1. Order 2 is formed by the convergence of two Order 1 tidal creeks, and so on for the remaining tidal creek orders. Tidal creek length is defined by the center line of tidal creeks. The sinuosity ratio provides information about tidal creek

curvature, as described in Eq. 5. The drainage ratio provides information about drainage efficiency, as described in Eq. 6.

$$r_s = L/L_e$$

5

$$r_d = L/A$$

6

where r_s represents the sinuosity ratio of the tidal creek, L is the length of the tidal creek, L_e represents the Euclidean distance from the starting point to the ending point of the tidal creek, r_s represents the drainage ratio of the tidal creek, and A is the area of the watershed in the salt marsh.

As a common spatial analysis function for the proximity analysis, buffer analysis was performed to determine the vegetation cover area on both sides of the tidal creeks. According to previous studies discussed in Fan et al. (2020), a 100 m buffer zone on tidal creeks is regarded as a suitable distance range to explore the relationship between tidal creek networks and invasive species distribution characteristics. The area covering a 100 m buffer zone around tidal creeks was calculated based on ArcGIS 10.6. The invasion ratio of *S. alterniflora* was calculated in Eq. 7 with a 100 m buffer zone around tidal creeks. The larger value of Mean(r) means a higher invasion in a certain zone. The expansion rate of *S. alterniflora* was also calculated, as shown in Eq. 8.

$$r_i = A/A_T$$

7

$$A_e = A_s \times (1+p)^N$$

8

where $r_{invasion}$ is the invasion ratio of the *S. alterniflora* in the certain invaded tidal creek, A is the area of *S. alterniflora*, A_T is the total area, p is the invasion rate, N is the number of years, and A_s and A_e show the areas of *S. alterniflora* at the start and end of the period, respectively.

4. Results

4.1 Spatiotemporal Dynamics of *S. Alterniflora* Invasion

The area of *S. alterniflora* is calculated with an accuracy rate of 88–97%, which means the results present an accurate expansion of invasive species and can be used for further spatiotemporal analysis.

Figure 4(a) presents the distribution of *S. alterniflora* in the JDS shoal from 2003 to 2021. According to the total area of *S. alterniflora* and using Sun et al. (2020) phase division, there are two phases of the *S. alterniflora* invasion process, including the initiation phase (1997–2010) and the expansion phase (2010–2021), as shown in Fig. 4(b). *S. alterniflora* first colonized the JDS shoal with a total area of 55 hm^2. During the initiation phase, *S. alterniflora* expanded at the center of the whole of the Zhongsha Shoal and the Xiasha Shoal and no *S. alterniflora* colonized Shangsha Shoal. The total area of *S. alterniflora* at the end of the initiation phase (1923.1 hm^2) was 35 times larger than that at the start of the initiation phase (55 hm^2). Figure 4 also shows that *S. alterniflora* spread northward, eastward, and north-eastward along the Shangsha Shoal; northward, westward, and north-westward along the Zhongsha Shoal; and northward, eastward, and north-eastward along the Xiasha Shoal in the expansion phase. The total area of *S. alterniflora* at the end of the expansion phase (6150.79 hm^2) was three times larger than that at the start of this phase (1923.1 hm^2). The total area kept increasing from 1997 to 2021, apart from during 2011 and 2013.

Figure 4 (located here)

4.2 Data Set Zonal Relationship Between Tidal Creek Networks and Invasive Species

To analyze the spatial relationship between the tidal creek network and the invasive species, JDS shoal is divided into three subareas from the northwest to the southeast, including six zones (Fig. 5(a)). Zone 1 belongs to the entrance zone of the Yangtze Estuary; Zones 2, 3, and 4 belong to the transition zones; and Zones 5 and 6 belong to the coastal zones.

As shown in Table 2, *S. alterniflora* invaded later in the Shangsha Shoal (Zones 1 and 2) than the Zhongsha Shoal and the Xiasha Shoal. Although *S. alterniflora* invaded the Shangsha Shoal after 2008 (which was later than other shoals), *S. alterniflora* shrank after its invasion in the Shangsha Shoal from 2008 to 2014, instead of expanding to other shoals. *S. alterniflora* accelerated its expansion between 2014 and 2017, and then expanded slowly between 2017 to 2020 in the Shangsha Shoal. Zone 1 still featured a substantial invasion of 0.18 in 2020, indicating the invasive species' potential for further expansion. The mean annual invasion rate of the invasive species in Zone 1 was larger than in Zone 2. This was because Zone 1 is at the entrance zone of the Yangtze Estuary and *S. alterniflora* had access to expand in the northern and the northwestern direction. The river between the Shangsha Shoal and the Zhongsha Shoal blocked its expansion in Zone 2. Owing to blocking effects, the mean annual invasion rate of vegetation in transition zones (Zones 2, 3, and 4) was smaller than in other zones, below 0.10. In addition, the annual invasion rate of *S. alterniflora* was larger in Zone 5 than in Zone 6, especially from 2002 to 2014, because Zone 5 occupied the larger area west of the Xiasha Shoal, which was the area of vegetation's initial expansion.

Table 2
Zonal annual invasion rate of *S. alterniflora* from 2002 to 2018

Year	Annual Invasion Rate of *S. alterniflora*					
	Zone 1	Zone 2	Zone 3	Zone 4	Zone 5	Zone 6
2002–2005	-	-	0.18	0.33	0.85	0.12
2005–2008	-	-	-0.05	-0.31	0.57	0.23
2008–2014	-0.28	-0.33	0.17	0.36	0.3	0.21
2014–2017	1.37	0.39	-0.02	-0.02	0.14	0.1
2017–2020	0.18	0.01	0.02	0.02	0.07	0.07
Mean	0.43	0.02	0.06	0.08	0.38	0.15

Figure 5 and Table 3 provide information on the spatial relationship between tidal creeks and *S. alterniflora* in different zones. In terms of geographical area, the invasive rate of *S. alterniflora* was the highest in 2017, reaching 0.59 in JDS shoal and 0.71 in Zone 4. Tidal creeks with a high r value were centrally located at the Zhongsha Shoal and the Xiasha Shoal. The Mean(r) of *S. alterniflora* was higher than 0.5 in Zones 3, 4, 5, and 6, with Zone 4 reaching 0.71. After 2017, there was a decreased invasive rate in the southeast of the Xiasha Shoal. From 2002 to 2020, *S. alterniflora* invaded later in the Shangsha Shoal than in the Zhongsha Shoal and the Xiasha Shoal. Tidal creek buffer zones were invaded in the large area at the center of the Zhongsha Shoal and the Xiasha Shoal. Moreover, the number of tidal creeks invaded by *S. alterniflora* grew year by year, except between 2005 and 2008.

Regarding the subarea, there was a significant difference in the spatial distribution of invasive tidal creeks among the partitions. At the entrance zone of the Yangtze Estuary (Zone 1), the number of invaded tidal creeks and the Mean(r) increased from 2014 to 2020. The coefficient of variation was smaller and the Mean(r) was larger in the year 2014 than in 2020, indicating that *S. alterniflora* would invade further. In the transition zones (Zones 2, 3, and 4), the number of invaded tidal creeks increased over the years; however, it decreased in Zones 3 and 4 from 2005 to 2008 and from 2017 to 2020. The Mean(r) fluctuated obviously in Zones 3 and 4. Compared with other transition zones, Zone 4 had a larger invasion rate and a smaller coefficient of variation and this phenomenon indicated that the conditions in Zone 4 are more suitable for the invasive plant's growth.

For the coastal zones, Zones 5 and 6 had the same invasion pattern and the invasion rate obtained the average level of six zones. Overall, from these subarea results, we predict that

the invasion of *S. alterniflora* will fluctuate in the transition zones and further expand at the entrance zone of the Yangtze Estuary and the coastal zone.

Figure 5 (located here)

Table 3
List of tidal creek number, mean invasion rate, standard deviation of invasion rate and coefficient of variation of invasion rate in different zones of JDS shoal in 2002, 2005, 2008, 2014, 2017 and 2020.

Year	Zone	Zone 1	Zone 2	Zone 3	Zone 4	Zone 5	Zone 6	JDS shoal
2002	TC number			22	60	11	35	128
	Mean (r)			0.17	0.23	0.04	0.15	0.18
	Standard deviation (r)			0.27	0.19	0.05	0.19	0.20
	Coefficient of variation (r)			1.61	0.84	1.44	1.25	1.14
2005	TC number		-	50	168	15	29	262
	Mean (r)		-	0.47	0.62	0.13	0.41	0.54
	Standard deviation (r)			0.35	0.31	0.16	0.35	0.34
	Coefficient of variation (r)			0.74	0.50	1.23	0.86	0.63
2008	TC number		2	26	92	34	39	193
	Mean (r)		0.02	0.41	0.51	0.35	0.28	0.42
	Standard deviation (r)		0.01	0.31	0.28	0.19	0.27	0.28
	Coefficient of variation (r)		0.74	0.76	0.55	0.54	0.96	0.68
2014	TC number	18	74	130	232	140	132	726
	Mean (r)	0.03	0.09	0.60	0.76	0.50	0.63	0.57
	Standard deviation (r)	0.03	0.15	0.29	0.22	0.30	0.37	0.34
	Coefficient of variation (r)	1.00	1.72	0.48	0.29	0.60	0.58	0.60
2017	TC number	30	70	162	289	181	199	931
	Mean (r)	0.13	0.16	0.52	0.71	0.57	0.69	0.59
	Standard deviation (r)	0.10	0.14	0.28	0.22	0.34	0.30	0.32
	Coefficient of variation (r)	0.76	0.91	0.52	0.31	0.60	0.43	0.54
2020	TC number	44	98	155	206	215	251	969
	Mean (r)	0.25	0.19	0.45	0.74	0.51	0.54	0.51
	Standard deviation (r)	0.15	0.16	0.25	0.25	0.27	0.30	0.30

Year	Zone	Zone 1	Zone 2	Zone 3	Zone 4	Zone 5	Zone 6	JDS shoal
	Coefficient of variation (r)	0.59	0.82	0.56	0.33	0.53	0.57	0.59

Figure 6 shows the length-grade boxplot of tidal creeks invaded by S. alterniflora in the initiation phase (2002, 2005, and 2008) and the expansion phase (2014, 2017, and 2020). The number of tidal creeks in 2002, 2005, and 2008 was 112, 223, and 177 with total lengths of 54 km, 83 km, and 103 km, respectively. In 2014, 2017, and 2020, there were 657, 849, and 896 tidal creeks with total lengths of 657 km, 849 km, and 896 km, respectively. From 2002 to 2008, the number of tidal creeks increased by 58.04% and the total length of tidal creeks increased by 90.74%. During the expansion phase, the number of tidal creeks increased by 36.38% and the total length of tidal creeks increased by 27.11%, indicating that the tidal creek expansion rate decreased from *S. alterniflora*'s initiation to the expansion phase. While Zone 6 had the most tidal creek numbers during the initiation and expansion phases, its length occupation decreased from 51.51–25.12%. Figure 9 indicates that the average tidal creek length decreased by 27.39% (Zone 2), 47.70% (Zone 3), 57.72% (Zone 4), 38.68% (Zone 5), and 29.91% (Zone 6). Owing to the ebb tide erosion

and the control of upstream branch tidal creeks, tidal creeks with low order evolved to high order; thus, the average tidal creek length decreased from the initiation to the expansion phase.

Figure 6 (located here)

The sinuosity ratio is a parameter that describes the curvature of tidal creeks. As shown in Fig. 7(a), the median sinuosity fluctuated from Zone 2 to Zone 6 in the range from 1.05 to 1.08 in the initiation phase. Zone 2 had the largest median sinuosity ratio (1.08), and Zone 1 and Zone 6 had the lowest median value of sinuosity ratio (1.05) in 2002, 2005, and 2008. During the expansion phase, the sinuosity ratio of Zone 2 increased to 1.07 in the median, and that in Zone 1 and Zone 6 decreased to 1.07 and 1.06, respectively, as shown in Fig. 7(b). This indicates that, during *S. alterniflora*'s invasion and expansion in JDS shoal, the curvature of the tidal creek system remained steady.

Figure 7 (located here)

4.3 Relationship Between Tidal Creek Networks and Invasive Species on the Large Scale

Figure 8 documents the characteristics of tidal creek networks (the median sinuosity ratio, drainage efficiency, and length) with the invasive area of 0–10, 10–20, 20–30, 30–40, and 40–50 hm^2. As shown in Fig. 8(a), the mean value of the sinuosity ratio stayed in the range between 1 and 1.2 from 2002 to 2020. The median sinuosity ratio of tidal creeks with a 10–20 hm^2 area was larger than those with a 20–30 hm^2 invasion area and 0–10 hm^2 area from 2005 to 2014. In 2014, tidal creeks with 30–40 hm^2 of *S. alterniflora* invasion had the largest sinuosity ratio, followed by 40–50 hm^2 and 10–20 hm^2. Between

2017 and 2020, the sinuosity ratio increased with the increase in invasion area. The drainage efficiency grew with the increase in the area of the invasive species. Figure 8(b) shows that the drainage efficiency stayed above 4×10^{-3} with a 10–50 hm^2 *S. alterniflora* area; it remained in the range of 3×10^{-3} to 4×10^{-3} with an *S. alterniflora* area of 0–10 hm^2. For the mean length, the shortest lengths were those with an area of 0–10 hm^2, which are below 500 m in Fig. 8(c). The longest tidal creeks were within a 20–30 hm^2 invasion area from 2005 to 2008 and a 40–50 hm^2 invasion area from 2014 to 2020.

Figure 8 (located here)

5. Discussion

The salt marsh covered by *S. alterniflora* is regarded as a “green desert”; this is because *S. alterniflora* competes with native plant species, reduces the diversity of intertidal benthic fauna, and negatively affects bird habitat quality. At the same time, it also forms biological dikes that affect tidal flat hydrological connectivity, leading to the degradation of seagrass beds and influencing coastal ecological functions (Qi et al. 2017; Sun et al. 2020). After its introduction into China in 1979, it aggressively invaded and rapidly expanded to coastal provinces and cities (Mao et al. 2019), affecting the morphological characteristics of coastal salt marshes.

The invasion of *S. alterniflora* has spatial differences at the landscape scale. Previous literature (Mao et al. 2019; Sun et al. 2020) recognizes that tidal creeks are corridors that promote invasion. This is a result of their spatial configuration, with highly connected networks. The dispersal of seeds of halophytes in salt marshes depends on tidal flow (Ayres et al. 2004). Our results show that the first expansion and invasion in the JDS Shoal was on both sides of the channel between the Zhongsha Shoal and the Xiasha Shoal (Fig. 4(a)), indicating that the tidal creek network promotes the invasion of *S. alterniflora* along the tidal channel. For the invading species expansion rate, the invasion period is divided into two phases, with the same discernibility value (0.75) as that of Sun et al. (2020) (Fig. 4(b)). The difference between the Yellow River Estuary and the JDS shoal is that one belongs to the floodplain in the estuary with the landward invasion of *S. alterniflora*, and one belongs to the estuary sandbar, where *S. alterniflora* expanded from the center to the outer area. The pattern of *S. alterniflora*’s invasion in the Shangsha Shoal was the same as in San Francisco Bay, where it invaded the intertidal salt marsh along the tidal creek network (Callaway and Josselyn 1992).

As an important geomorphological element of tidal flats, tidal creeks form in the intertidal zone and are the main channel for transporting water, sand materials, and energy to the upper part of tidal flats (Fitch et al. 2009). The tidal creek network is the most active geomorphic structure to link the ocean and coastal wetland (Fagherazzi and Furbish 2001; L. Zhao et al. 2019). The length, sinuosity ratio, drainage efficiency, and length are important parameters to describe the tidal creek network. At the initiation phase, the sinuosity ratio decreased with the increasing invasion area from 10 hm^2 to 20 hm^2 when the morphological characteristics of the tidal creek were controlled by native vegetation. A previous study (Fan et al. 2020) shows that the tidal creek’s curvature distribution of *S. alterniflora* is lower than that of

native species. The same phenomenon (Kearney and Fagherazzi 2016; C. Schwarz et al. 2014; Vandenbruwaene et al. 2011)—which is that curvature increases with the increasing cover of vegetation—was also found in this study during the expansion phase of *S. alterniflora*. The overall length decreased because the tidal creek developed to higher orders. The drainage efficiency decreased with 10–30 hm^2 covering the area of invaded species, as shown in Fig. 8(b). Because *S. alterniflora* has stiff stems and a large canopy, it increases the drag force and accelerates sediment settling velocity, which leads to a more rapid expansion of the tidal prism and a decline in drainage efficiency. The increase in drainage ratio occurred in a 30–50 hm^2 invasion area with tidal meandering. The same phenomenon is found in the literature(Allen 2000; Cahoon 2009).

Our research established that the invasion of *S. alterniflora* influences the morphology of salt marshes, especially the development of tidal creek networks. This effect of invasive species had spatial differences, which were related to the location of JDS shoal. JDS shoal is a sand bar in an estuary of the Yangtze River. The range of vegetation expansion in the past two decades is consistent with the trend of sand body changes between 1960 and 2020: these have expanded in southern and eastern directions. Owing to the deposition of the Shangsha Shoal, less *S. alterniflora* invaded. It remains to be seen whether the change process of invasive vegetation expansion in the future is consistent with the change of sand bodies in the past two decades.

6. Conclusion

Through remote sensing images, this study analyzed the influence of *S. alterniflora* on morphological evolution. This research found that the total area of *S. alterniflora* at the end of the initiation phase (1923.1 hm2) was 35 times larger than that at the start of the initiation phase (55 hm2). There was a spatial difference in *S. alterniflora*'s invasion in JDS shoal, reflecting that invasion of *S. alterniflora* occurred after 2010 in Shangsha Shoal from the outer shoal. *S. alterniflora* invaded from the center to the outer shoal in the Zhongsha Shoal and the Xiasha Shoal. Additionally, with the influence of plant invasion, median tidal creek lengths decreased and the median tidal creek sinuosity ratio remained stable between 1.06 and 1.07 in the subarea. Based on the discussion, the range of vegetation expansion in the past two decades is consistent with the trend of sand body changes between 1960 and 2020, an expansion in southern and eastern directions. In recent years, the invasion of *S. alterniflora* in the upper part of the Shangsha Shoal has accelerated. It remains to be seen whether the change process of invasive vegetation expansion in the future is consistent with the change of sand bodies in the past two decades.

To our knowledge, this is the first study to quantitatively analyze the spatiotemporal effects of invasive species on salt marsh morphology. This research provides data that will enrich and complete the theoretical system of bio-geomorphology of salt marsh wetlands and provide a scientific suggestion for wetland ecological conservation and restoration.

Declarations

Conflict of Interest

The authors declare that the research was conducted in the absence of any commercial or financial relationships that could be construed as a potential conflict of interest.

Author Contributions

XW: Conceptualization, data analysis, and writing-original draft. XP: resources, supervision, revise and editing. HZ: conceptualization, supervision, revise and editing; LZ: field investigation and revise the manuscript. CL: preprocess remote image and editing. All authors contributed to the article and approved the submitted version.

Funding

This study was supported by the National Natural Science Foundation of China (grant U2040204), the Jiangsu Provincial Natural Science Foundation of China (grant BK2020020) and the Open Research Fund of Key Laboratory of Estuarine & Coastal Engineering, Ministry of Transport (grant KLECE202301).

Acknowledgements

The authors are grateful to the Shanghai Estuarine and Coastal Research Centre for furnishing bathymetry data of the Yangtze Estuary. The authors would also like to thank the Ministry of Transport in Shanghai Estuarine and Coastal Science Research Centre for their support in the data collection and field investigation.

References

1. Allen, J. R. L. 2000. Morphodynamics of holocene salt marshes: a review sketch from the Atlantic and Southern North Sea coasts of Europe. *Quaternary Science Reviews,* 19: 1839-1840.
2. An, S. Q., Gu, B. H., Zhou, C. F., Wang, Z. S., Deng, Z. F., Zhi, Y. B., . . . Liu, Y. H. 2007. Spartina invasion in China: implications for invasive species management and future research. *Weed Research,* 47: 183-191.
3. Ayres, D. R., Smith, D. L., Zaremba, K., Klohr, S., & Strong, D. R. 2004. Spread of Exotic Cordgrasses and Hybrids (Spartina sp.) in the Tidal Marshes of San Francisco Bay, California, USA. *Biological Invasions,* 6: 221-231.
4. Bouma, T. J., De Vries, M. B., Low, E., Peralta, G., Tánczos, I. C., van de Koppel, J., & Herman, P. M. J. 2005. Trade-offs related to ecosystem engineering: a case study on stiffness of emerging macrophytes. *Ecology,* 86: 2187-2199.
5. Cahoon, D. (2009). *Coastal Wetlands An Integrated Ecosystem Approach*.
6. Callaway, J. C., & Josselyn, M. N. 1992. The introduction and spread of smooth cordgrass (Spartina alterniflora) in South San Francisco Bay. *Estuaries,* 15: 218-226.

7. Chen, Z., Li, B., Zhong, Y., & Chen, J. 2004. Local competitive effects of introduced Spartina alterniflora on Scirpus mariqueter at Dongtan of Chongming Island, the Yangtze River estuary and their potential ecological consequences. *Hydrobiologia,* 528: 99-106.
8. D'Alpaos, A. 2011. The mutual influence of biotic and abiotic components on the long-term ecomorphodynamic evolution of salt-marsh ecosystems. *Geomorphology,* 126: 269-278.
9. D'Alpaos, A., Lanzoni, S., Mudd, S. M., & Fagherazzi, S. 2006. Modeling the influence of hydroperiod and vegetation on the cross-sectional formation of tidal channels. *Estuarine Coastal and Shelf Science,* 69: 311-324.
10. Davis, C. C., Willis, C. G., Connolly, B., Kelly, C., & Ellison, A. M. 2015. Herbarium records are reliable sources of phenological change driven by climate and provide novel insights into species' phenological cueing mechanisms. *American Journal of Botany,* 102: 1599-1609.
11. Fagherazzi, S., & Furbish, D. J. 2001. On the shape and widening of salt marsh creeks. *Journal of Geophysical Research: Oceans,* 106: 991-1003.
12. Fan, Y., Zhou, D., Ke, Y., Wang, Y., Wang, Q., & Zhang, L. 2020. Quantifying the correlated spatial distributions between tidal creeks and coastal wetland vegetation in the Yellow River Estuary. *Wetlands,* 40: 2701-2711.
13. Fei, S., Phillips, J., & Shouse, M. 2014. Biogeomorphic impacts of invasive species. *Annual Review of Ecology, Evolution, and Systematics,* 45: 69-87.
14. Fitch, R., Theodose, T., & Dionne, M. 2009. Relationships among upland development, nitrogen, and plant community composition in a maine salt marsh. *Wetlands,* 29: 1179-1188.
15. Frenkel, R. E., & Boss, T. R. 1988. Introduction, establishment and spread ofSpartina patens on Cox Island, siuslaw Estuary, Oregon. *Wetlands,* 8: 33-49.
16. Ge, Z., Cao, H., & Zhang, L. 2013. A process-based grid model for the simulation of range expansion of Spartina alterniflora on the coastal saltmarshes in the Yangtze Estuary. *Ecological Engineering,* 58: 105-112.
17. Gong, Z., Mou, K., Wang, Q., Qiu, H., Zhang, C., & Zhou, D. 2021. Parameterizing the Yellow River Delta tidal creek morphology using automated extraction from remote sensing images. *Science of the Total Environment,* 769: 144572.
18. Gorelick, N., Hancher, M., Dixon, M., Ilyushchenko, S., Thau, D., & Moore, R. 2017. Google Earth Engine: Planetary-scale geospatial analysis for everyone. *Remote Sensing of Environment,* 202: 18-27.
19. Goss-Custard, J. D., & Moser, M. E. 1988. Rates of change in the numbers of Dunlin, Calidris alpina, Wintering in British Estuaries in relation to the spread of Spartina anglica. *Journal of Applied Ecology,* 25: 95-109.
20. Goulden, M. L., Litvak, M., & Miller, S. D. 2007. Factors that control typha marsh evapotranspiration. *Aquatic Botany,* 86: 97-106.
21. Horton, R. E. 1945. Erosional development of streams and their drainage basins; hydrophysical approach to quantitative morphology. *GSA Bulletin,* 56: 275-370.

22. Huang, H., & Zhang, L. 2007. A study of the population dynamics of Spartina alterniflora at Jiuduansha shoals, Shanghai, China. *Ecological Engineering,* 29: 164-172.
23. Hubbard, J. C. E., & Partridge, T. R. 1981. Tidal immersion and the growth of Spartina anglica marshes in the Waihopai River Estuary, New Zealand. *New Zealand Journal of Botany,* 19: 115-121.
24. Jimenez, K. L., Starr, G., Staudhammer, C. L., Schedlbauer, J. L., Loescher, H. W., Malone, S. L., & Oberbauer, S. F. 2012. Carbon dioxide exchange rates from short- and long-hydroperiod Everglades freshwater marsh. *Journal of Geophysical Research: Biogeosciences,* 117.
25. Kakeh, N., Coco, G., & Marani, M. 2016. On the morphodynamic stability of intertidal environments and the role of vegetation. *Advances in Water Resources,* 93: 303-314.
26. Kearney, W. S., & Fagherazzi, S. 2016. Salt marsh vegetation promotes efficient tidal channel networks. *Nature Communications,* 7: 12287.
27. Kennish, M. J. 2001. Coastal salt marsh systems in the U.S.: a review of anthropogenic impacts. *Journal of Coastal Research,* 17: 731-748.
28. Kirwan, M., & Megonigal, P. 2013. Tidal wetland stability in the face of human impacts and sea-level rise. *Nature,* 504: 53-60.
29. Lao, C., Xin, P., Zuo, Y., & Cheng, H. 2022. Effect of fractional vegetation cover on the evolution of tidal creeks of the Jiuduansha shoal in Yangtze River Estuary (China) during 1996-2020. *Advances in Water Science,* 33: 15-26.
30. Li, B., Liao, C., Zhang, X., Chen, H., Wang, Q., Chen, Z., . . . Chen, J. 2009. Spartina alterniflora invasions in the Yangtze River estuary, China: An overview of current status and ecosystem effects. *Ecological Engineering,* 35: 511-520.
31. Ma, Z., Gan, X., Choi, C., Jing, K., Tang, S., Li, B., & Chen, J. 2007. Wintering bird communities in newly-formed wetland in the Yangtze River estuary. *Ecological Research,* 22: 115-124.
32. Mao, D., Liu, M., Wang, Z., Li, L., Man, W., Jia, M., & Zhang, Y. 2019. Rapid invasion of Spartina alterniflora in the coastal zone of mainland China: Spatiotemporal patterns and human prevention. *Sensors,* 19: 2308.
33. Marani, M., Lanzoni, S., Zandolin, D., Seminara, G., & Rinaldo, A. 2002. Tidal meanders. *Water Resources Research,* 38: 7-1-7-14.
34. Mcleod, E., Chmura, G. L., Bouillon, S., Salm, R., Björk, M., Duarte, C. M., . . . Silliman, B. R. 2011. A blueprint for blue carbon: toward an improved understanding of the role of vegetated coastal habitats in sequestering CO2. *Frontiers in Ecology and the Environment,* 9: 552-560.
35. Neubauer, S. C. 2008. Contributions of mineral and organic components to tidal freshwater marsh accretion. *Estuarine, Coastal and Shelf Science,* 78: 78-88.
36. Nyman, J. A., Walters, R. J., Delaune, R. D., & Patrick, W. H. 2006. Marsh vertical accretion via vegetative growth. *Estuarine, Coastal and Shelf Science,* 69: 370-380.
37. Qi, M., Sun, T., Zhang, H., Zhu, M., Yang, W., Shao, D., & Voinov, A. 2017. Maintenance of salt barrens inhibited landward invasion of Spartina species in salt marshes. *Ecosphere,* 8: e01982.

38. Quan, W., Shi, L., & Chen, Y. 2011. Comparison of nekton use for cordgrass Spartina alterniflora and Bulrush scirpus mariqueter marshes in the Yangtze River Estuary, China. *Estuaries and Coasts,* 34: 405-416.
39. Quan, W., Zhang, H., Wu, Z., Jin, S., Tang, F., & Dong, J. 2016. Does invasion of Spartina alterniflora alter microhabitats and benthic communities of salt marshes in Yangtze River estuary? *Ecological Engineering,* 88: 153-164.
40. Rosso, P. H., Ustin, S. L., & Hastings, A. 2006. Use of lidar to study changes associated with Spartina invasion in San Francisco Bay marshes. *Remote Sensing of Environment,* 100: 295-306.
41. Schwarz, C., Ye, Q. H., van der Wal, D., Zhang, L. Q., Bouma, T., Ysebaert, T., & Herman, P. M. J. 2014. Impacts of salt marsh plants on tidal channel initiation and inheritance. *Journal of Geophysical Research-Earth Surface,* 119: 385-400.
42. Schwarz, C., Ysebaert, T., Vandenbruwaene, W., Temmerman, S., Zhang, L., & Herman, P. M. J. 2016. On the potential of plant species invasion influencing bio-geomorphologic landscape formation in salt marshes. *Earth Surface Processes and Landforms,* 41: 2047-2057.
43. Sheehan, M. R., & Ellison, J. C. 2014. Intertidal morphology change following Spartina anglica introduction, Tamar Estuary, Tasmania. *Estuarine, Coastal and Shelf Science,* 149: 24-37.
44. Strayer, D. L., Eviner, V. T., Jeschke, J. M., & Pace, M. L. 2006. Understanding the long-term effects of species invasions. *Trends in Ecology & Evolution,* 21: 645-651.
45. Sun, L., Shao, D., Xie, T., Gao, W., Ma, X., Ning, Z., & Cui, B. 2020. How does Spartina alterniflora invade in salt marsh in relation to tidal channel networks? patterns and processes. *Remote Sensing,* 12: 2983.
46. Theoharides, K. A., & Dukes, J. S. 2007. Plant invasion across space and time: factors affecting nonindigenous species success during four stages of invasion. *New Phytologist,* 176: 256-273.
47. van Hulzen, J. B., van Soelen, J., & Bouma, T. J. 2007. Morphological variation and habitat modification are strongly correlated for the autogenic ecosystem engineer Spartina anglica (common cordgrass). *Estuaries and Coasts,* 30: 3-11.
48. Vandenbruwaene, W., Temmerman, S., Bouma, T. J., Klaassen, P. C., de Vries, M. B., Callaghan, D. P., . . . Meire, P. 2011. Flow interaction with dynamic vegetation patches: Implications for biogeomorphic evolution of a tidal landscape. *Journal of Geophysical Research: Earth Surface,* 116.
49. Wang, F., Sanders, C. J., Santos, I. R., Tang, J., Schuerch, M., Kirwan, M. L., . . . Li, Z. a. 2020. Global blue carbon accumulation in tidal wetlands increases with climate change. *National Science Review,* 8.
50. Wang, S., Chen, F., Meng, Y., & Zhu, Q. 2021. Spatiotemporal Distribution Characteristics of Nutrients in the Drowned Tidal Inlet under the Influence of Tides: A Case Study of Zhanjiang Bay, China. *International Journal of Environmental Research and Public Health,* 18: 2089.
51. Wu, W., Yang, Z., Tian, B., Huang, Y., Zhou, Y., & Zhang, T. 2018. Impacts of coastal reclamation on wetlands: Loss, resilience, and sustainable management. *Estuarine, Coastal and Shelf Science,* 210: 153-161.

52. Wu, Y., Liu, J., Yan, G., Zhai, J., Cong, L., Dai, L., . . . Zhang, M. 2020. The size and distribution of tidal creeks affects salt marsh restoration. *Journal of Environmental Management,* 259: 110070.
53. Xiao, D., Zhang, L., & Zhu, Z. 2010. The range expansion patterns of Spartina alterniflora on salt marshes in the Yangtze Estuary, China. *Estuarine, Coastal and Shelf Science,* 88: 99-104.
54. Xin, P., Wilson, A., Shen, C., Ge, Z., Moffett, K. B., Santos, I. R., . . . Barry, D. A. 2022. Surface water and groundwater interactions in salt marshes and their impact on plant ecology and coastal biogeochemistry. *Reviews of Geophysics,* 60: 1-54.
55. Yang, S., Li, H., Ysebaert, T., Bouma, T. J., Zhang, W., Wang, Y., . . . Ding, P. 2008. Spatial and temporal variations in sediment grain size in tidal wetlands, Yangtze Delta: On the role of physical and biotic controls. *Estuarine Coastal and Shelf Science,* 77: 657-671.
56. Zhao, B., Liu, Y., Xu, W., Liu, Y., Sun, J., & Wang, L. 2019. Morphological characteristics of tidal creeks in the central coastal region of Jiangsu, China, using LiDAR. *Remote Sensing,* 11: 2426.
57. Zhao, L., Xin, P., Cheng, H., & Chu, A. 2022. Combined effects of river discharge regulation and estuarine morphological evolution on salinity dynamics in Yangtze Estuary, China. *Estuarine, Coastal and Shelf Science,* 276: 108002.
58. Zhao, L., Xu, C., Ge, Z., van de Koppel, J., & Liu, Q. 2019. The shaping role of self-organization: linking vegetation patterning, plant traits and ecosystem functioning. *Proceedings of the Royal Society B: Biological Sciences,* 286: 20182859.
59. Zhu, Z., Zhang, L., Wang, N., Schwarz, C., & Ysebaert, T. 2012. Interactions between the range expansion of saltmarsh vegetation and hydrodynamic regimes in the Yangtze Estuary, China. *Estuarine, Coastal and Shelf Science,* 96: 273-279.

Figures

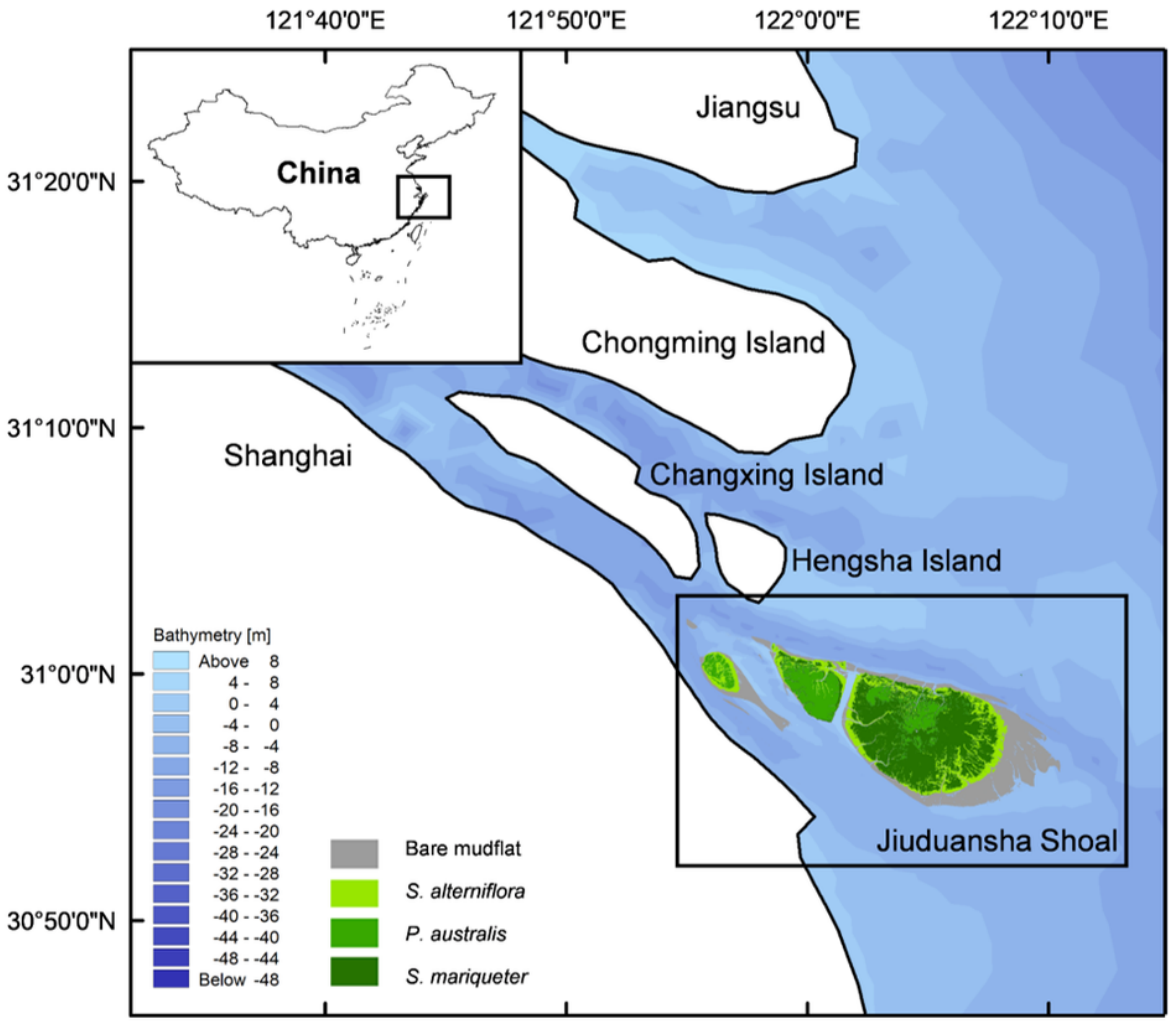


Figure 1

The location of the JDS Shoal, the Yangtze Estuary

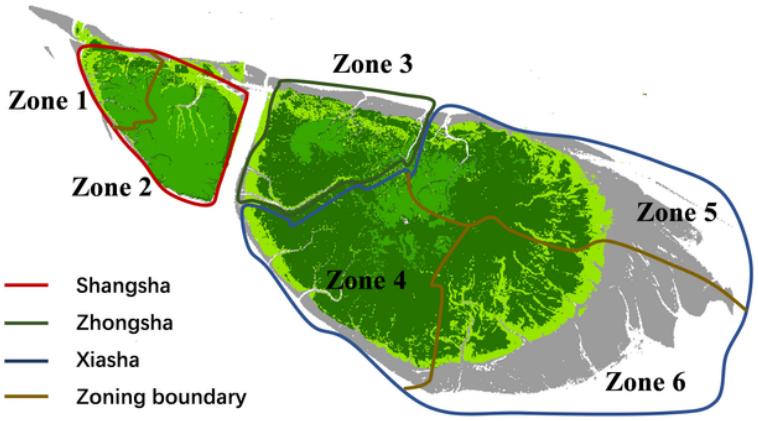


Figure 2

The division of the JDS Shoal into the Shangsha Shoal, Zhongsha Shoal and Xiasha Shoal, as well as the boundary of the zoning of the JDS Shoal

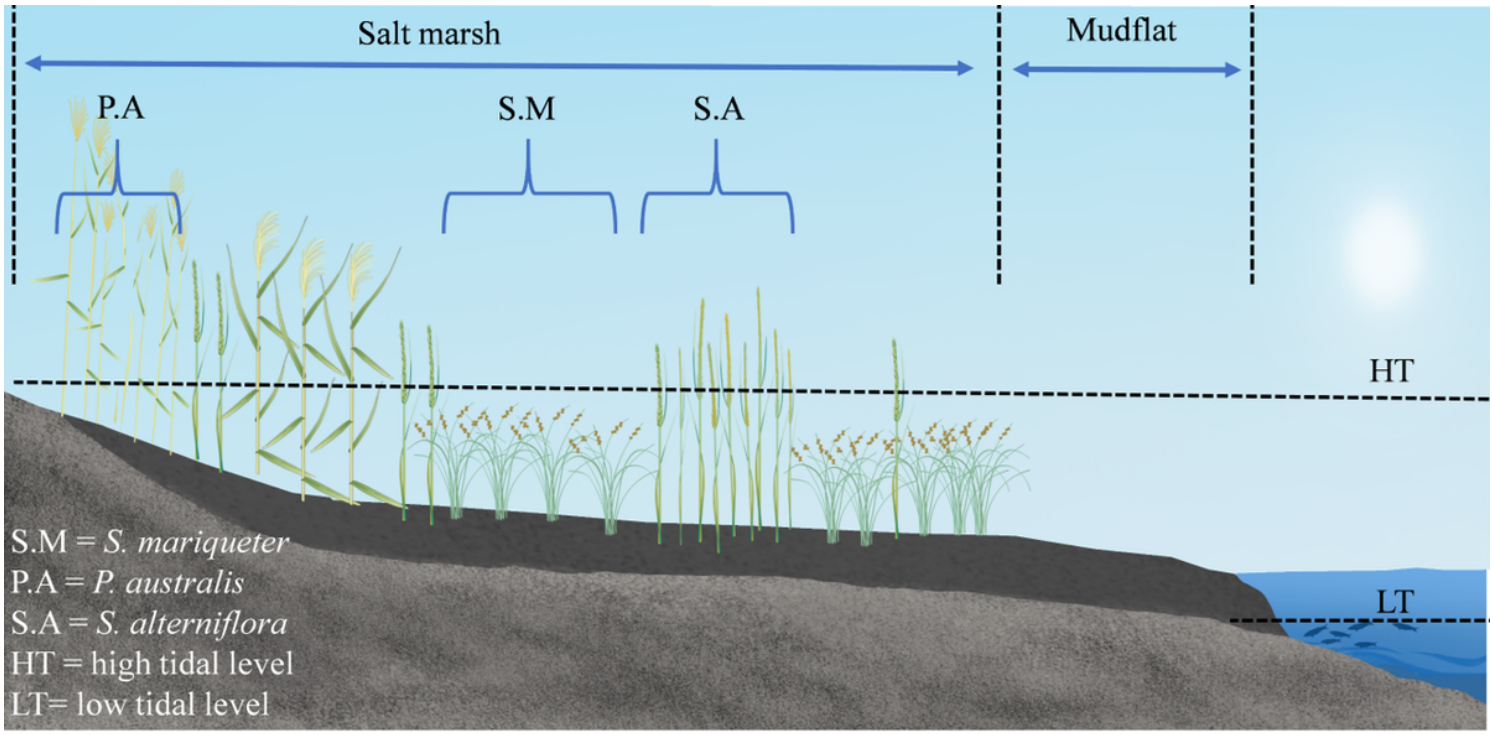


Figure 3

Mature mudflat and saltmarsh zonation within the coastal wetland, modified from S. Wang et al. (2021)

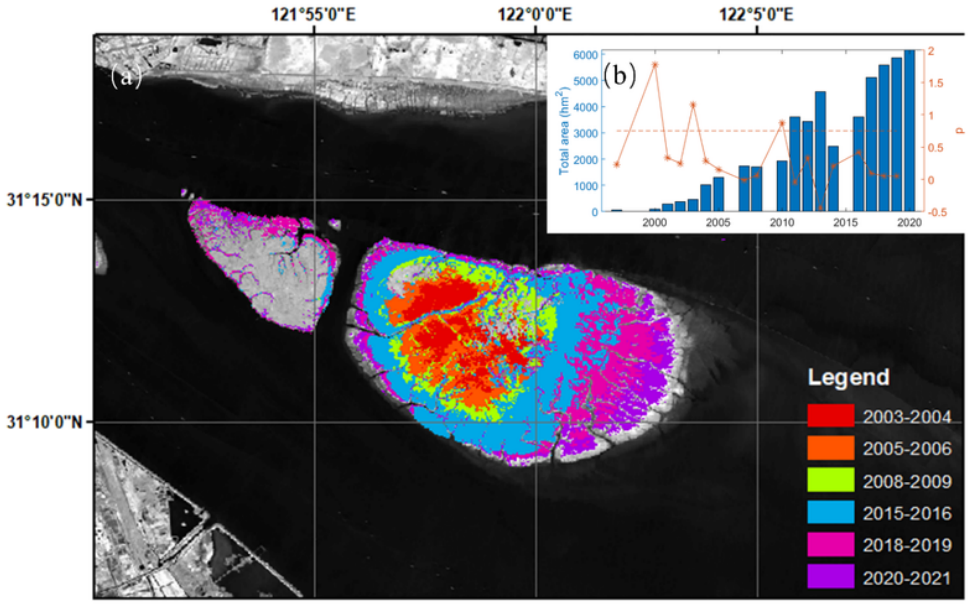


Figure 4

The distribution of *S. alterniflora*invasion and expansion in the Jiuduansha Shoal, based on the remote sensing images from 2003 to 2021 (a); Time series of *S. alterniflora* total area and its expansion rate from 1997 to 2000 (b)

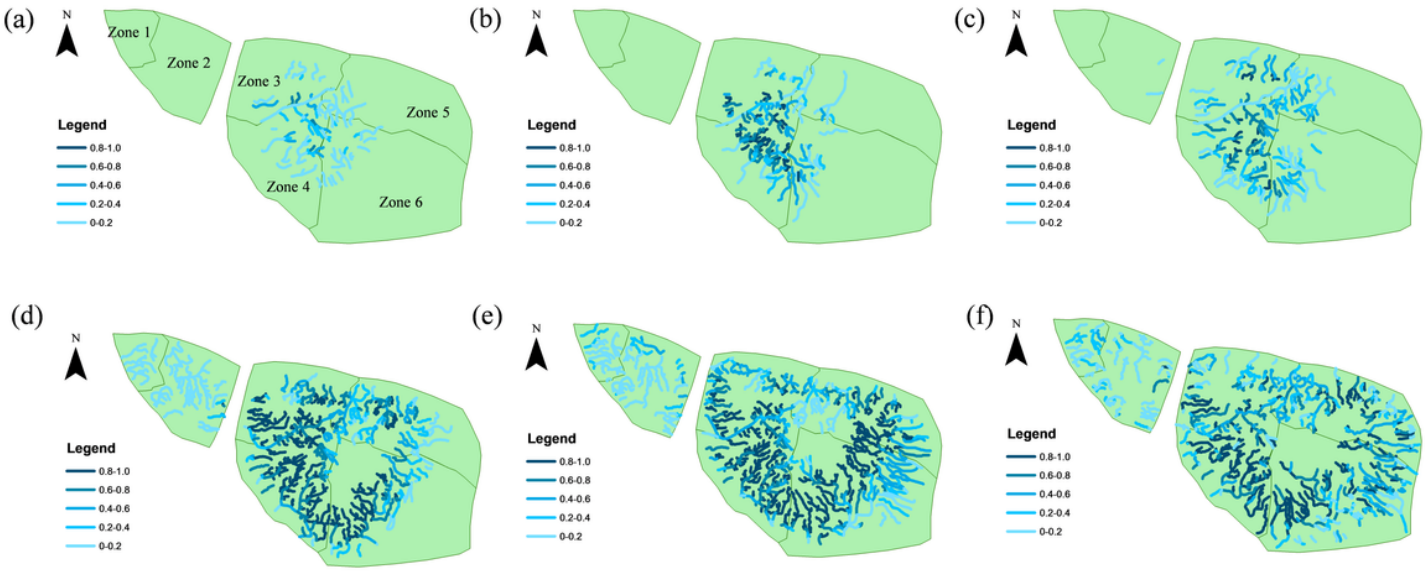


Figure 5

Spatial distribution of *S. alterniflora*'s invasion rate in the JDS shoal in 2002 (a), 2005 (b), 2008 (c), 2014 (d), 2017 (e) and 2020 (f)

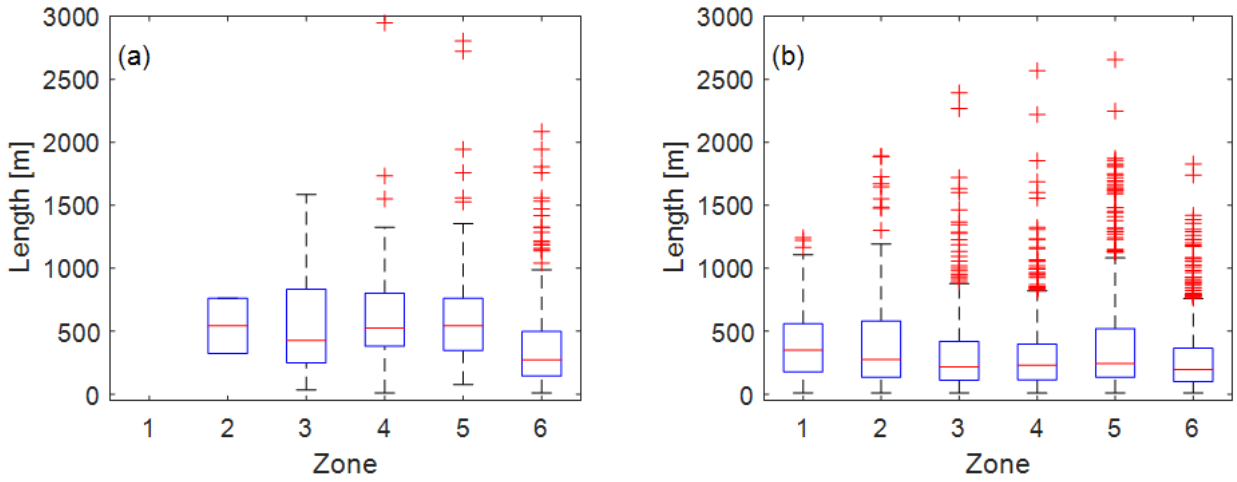


Figure 6

Length-grade boxplot of the invaded tidal creeks in (a) 2002, 2005, 2008, (b) 2014, 2017 and 2020

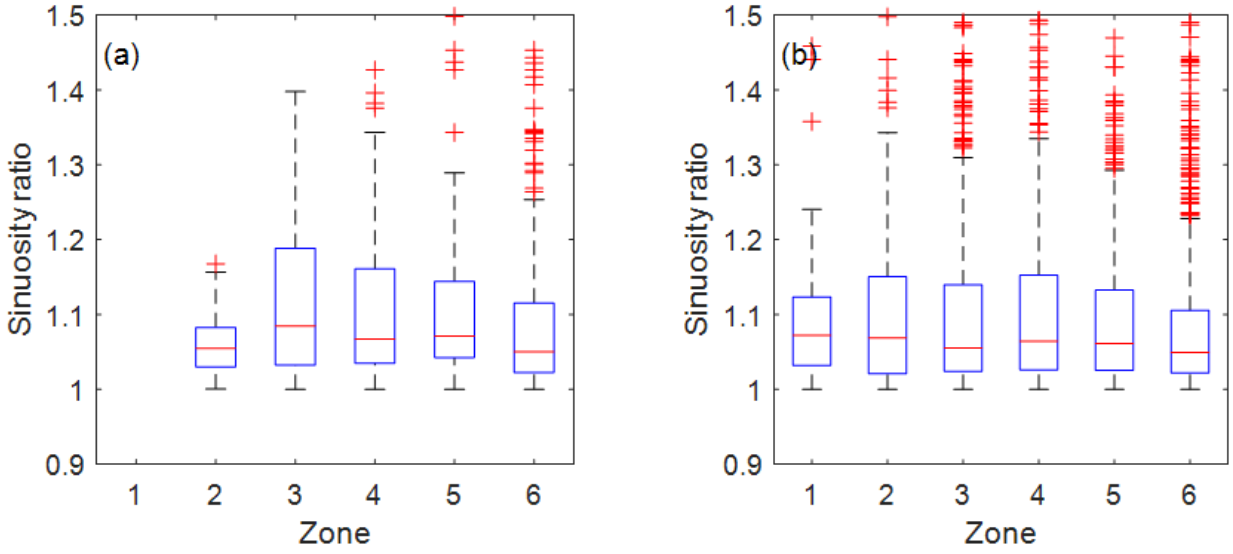


Figure 7

Sinuosity ratio-grade boxplot of the invaded tidal creeks in (a) 2002, 2005, 2008, (b) 2014, 2017 and 2020

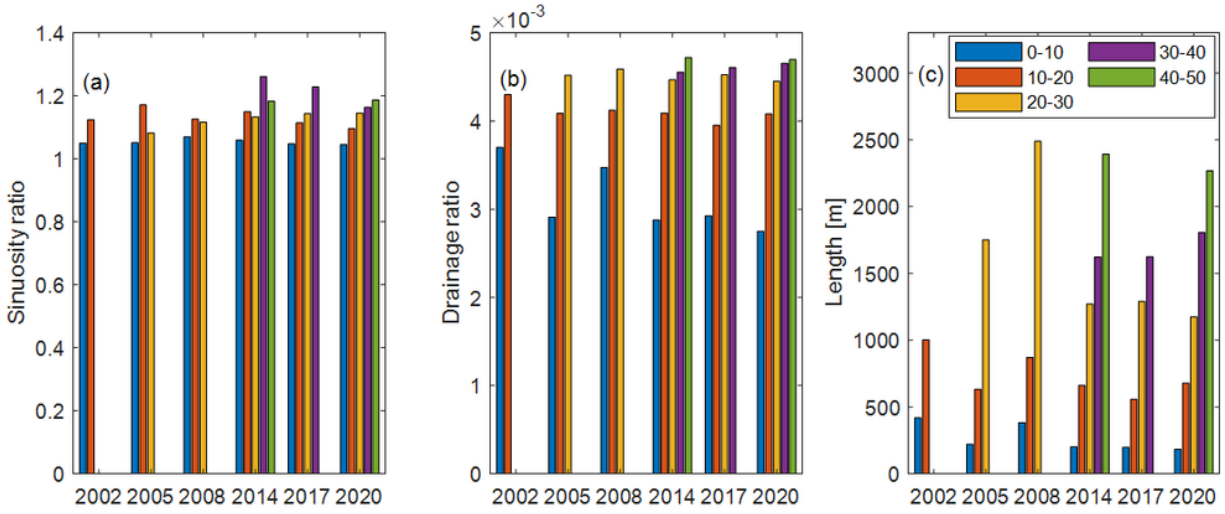


Figure 8

The median sinuosity ratio (a), drainage ratio (b) and length (c) of tidal creek in invasive area of 0-10, 10-20, 20-30, 30-40 and 40-50 hm^2